Design of a Power Factor Measurement System for Nonlinear Load

Md. Rifat Shahriar* · Ui-Pil Chong**

Abstract

This paper introduces and develops an efficient method for measuring power factor (PF) and its nature under nonlinear load current situations. The method is based on generating a pulse width modulated signal whose width correlates to the value of PF. This signal can then be employed as a feedback signal for controlling PF related power quantities in a system. This method has the advantages of its simple implementation, less computational complexity, and its allowable error of less than 4[%], which is justified by the computer simulation results.

Key Words : Nonlinear Load Current, True Power Factor, Microcontroller, Pulse Width Modulated Wave

1. Introduction

Accurate measurements of power factors (PF) under nonlinear load currents merit increased attention due to the popularity and the growing numbers of uses for nonlinear loads and power saving devices in recent decades[1-3]. Acquisition of PF information is essential in many applications: power quality management, calculations of apparent power requirements and controlling the PF of a load system are examples. Precise measurements of PF under

* Main author : Univ. of Ulsan, School of Electrical Eng.
** Corresponding author : Univ. of Ulsan, School of Electrical Eng.
   Tel : +82-52-259-2220
   E-mail : upchong@ulsan.ac.kr
   Date of submit : 2011. 9. 15
   First assessment : 2011. 10. 20
   Second : 2011. 10. 25
   Third : 2011. 11. 9
   Completion of assessment : 2011. 11. 15

non-sinusoidal environments are needed at this time.

The most conventional approach to measuring PF is the use of an electromechanical power factor meter [4] which is only accurate for the sinusoidal case [5]. A number of analog electronic circuits for PF measurement are proposed in [6-9]; however, these systems are incapable of determining lead/lag discrimination of a PF nature. Another approach to measuring PF is reported in [10] which is only developed for sinusoidal cases.

Several techniques and algorithms for true PF measurement based on Discrete Fourier Transform (DFT) or its computationally efficient implementation named Fast Fourier Transform (FFT) are proposed in [11-14]. They are also followed by the commercial PF measurement equipment [15]. However, this DFT-based approach may be erroneous due to aliasing, picket-fence effects, and

leakage which are analyzed and detailed in [16]. Measurement methods proposed in [17–18] based on wavelets are claimed to be successful, but their measurements and computations are considerably complex and their efficiency is highly dependent on the type of mother wavelet [19]. The least square algorithm based measurement method of electrical quantities is suggested in [19], which stated that this method is efficient, but that it requires the processing power of a DSP chip.

In this paper, we have developed a simple and computationally efficient method for real-time measurements of PF under nonlinear load current conditions. A system has been proposed that is capable of measuring a PF value and its nature from zero PF lagging through unity PF up to zero PF leading – contrasted to some of the early systems proposed in [6–9]. Unlike the commercial equipment available for this purpose [15], the proposed method does not require complex computations like those included in harmonic analysis. Basically, our method is based on a mixed-signal analysis approach, which outputs PF information in the form of a pulse width of a digital signal. Thus, a simplified implementation of the method proves its competitiveness with existing systems while computer simulation results guarantee its accuracy.

2. Power Factor Definition

Electric utilities generate and distribute nearly perfect fundamental sinusoidal voltages as reported in [30]. This fact, considered in [7, 18, 20, 33], is also verified in [31, 32] by case study and experimental results. Thus, obtained voltage waveform can be simply expressed as

$$v(t) = \sqrt{2}\,V_{rms}\sin(\omega t). \tag{1}$$

Considering the dc component in a steady state nonlinear load current, it can be expressed as

$$i(t) = I_0 + i_1(t) + \sum_{n=2}^{\infty} i_n(t). \tag{2}$$

Where I_0 is the dc component, $i_1(t)$ is the fundamental component and $i_n(t)$ is the component at the nth harmonic frequency. Equation (2) can also be expressed as

$$i(t) = I_0 + \sqrt{2}\,I_1\sin(\omega t + \theta_1) + \sum_{n=2}^{\infty} I_n\sin(n\omega t + \theta_n). \tag{3}$$

Where I_1, I_n are the rms values and θ_1, θ_n are the phase of load current at the fundamental and the nth-order harmonic respectively. The average power P can be expressed as [21–23]

$$P = \frac{1}{T}\int_0^T p(t)dt = \frac{1}{T}\int_0^T v(t)i(t)dt = V_{rms}I_1\cos(\theta_1). \tag{4}$$

According to the power triangle [24] apparent power can be expressed as

$$S = V_{rms}I_{rms}. \tag{5}$$

Power factor (PF) is generally defined as the ratio of the Real power (P) to the Apparent power (S) [21–23, 25].

$$PF = \frac{P}{S} = \frac{V_{rms}I_1\cos(\theta_1)}{V_{rms}I_{rms}} = \frac{I_1}{I_{rms}}\cos(\theta_1) \tag{6}$$

The ratio of I_1 to I_{rms} is known as distortion power factor which indicates how the harmonic distortion of a load current decreases the average power transferred to the load [21].

$$\mathrm{Distortion\,Power\,Factor} = \frac{I_1}{I_{rms}} \qquad (7)$$

The cosine of the phase angle between voltage and current $\cos(\theta_1)$ is defined as the displacement power factor (DPF) [21, 23, 26].

$$DPF = \cos(\theta_1) \qquad (8)$$

Therefore, the representation of PF in case of a nonlinear load current situation is

$$PF = \frac{I_1}{I_{rms}} DPF. \qquad (9)$$

The definition of PF expressed by (9) [7, 21, 23] is also known as "True PF" [3].

When the load is linear, load current $i(t)$ becomes pure sinusoidal and can be expressed as

$$i(t) = \sqrt{2}\,I_1 \sin(\omega t + \theta_1). \qquad (10)$$

In this case I_1 and I_{rms} become equal. Consequently, the expression in (9) becomes

$$PF = DPF = \cos(\theta_1). \qquad (11)$$

Note that the expression of (11) is appropriate only for sinusoidal load current conditions.

3. Development and Analysis of Proposed Scheme

A block diagram of the proposed method for measuring PF is shown in Fig. 1. Here a current transformer is used for measuring the nonlinear load current $i(t)$ which is then applied to the input of a narrow band filter to extract the fundamental component $i_1(t)$. Narrow band filters of higher orders usually consist of cascaded second order

band pass filters that use the Sallen-Key or the Multiple Feedback topology. A general transfer function of a second-order filter is [27]

$$A(s) = \frac{\frac{A_m}{Q}\cdot s}{1 + \frac{1}{Q}\cdot s + s^2} \qquad (12)$$

Here, the complex frequency variable $s = \sigma + j\Omega$; σ = damping factor, A_m= the gain at mid frequency and Q = quality factor.

Quality factor Q is defined as the ratio of the mid frequency (f_m) to the bandwidth (B).

$$Q = \frac{f_m}{B} = \frac{f_m}{f_2 - f_1} = \frac{1}{\Omega_2 - \Omega_1} = \frac{1}{\Delta\Omega} \qquad (13)$$

In (13) $\Omega_2 = \frac{f_2}{f_m}$ and $\Omega_1 = \frac{f_1}{f_m}$ are the normalized frequencies at lower and upper −3[db] points of pass band and $\Delta\Omega$ is normalized bandwidth. Q represents the selectivity of a band pass filter; a rising Q value results in stepper frequency response.

Between the two topologies for narrow band filters mentioned above, Multiple Feedback topology has advantages over the Sallen-Key due to the fact that it allows a designer to adjust Q, A_m, and f_m independently [27].
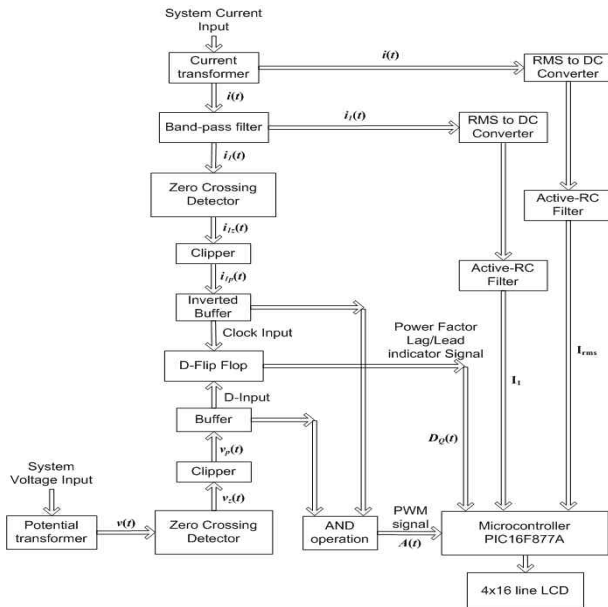
Fig. 1. Overview of the designed system for PF Measurement

A second order active band pass filter implemented by multiple feedback topology is shown in Fig. 2 which has the following transfer function.

$$A(s) = \cfrac{-\dfrac{R_2 R_3}{R_1 + R_3} C\,\omega_m \cdot s}{1 + \dfrac{2R_1 R_3}{R_1 + R_3} C\,\omega_m \cdot s + \dfrac{R_1 R_2 R_3}{R_1 + R_3} C^2\,\omega_m^2 \cdot s^2} \tag{14}$$
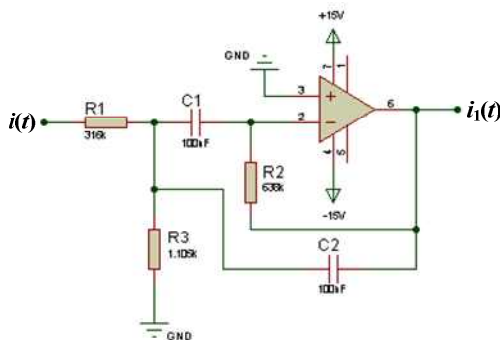

Fig. 2. Circuit diagram of Multiple Feedback band-pass filter (here, C1 = C2 = C)

After comparing coefficients of (14) with that of

(12) and using (13), the following expressions of filter design parameters can be obtained.

$$f_m = \frac{1}{2\pi C}\sqrt{\frac{R_1 + R_3}{R_1 R_2 R_3}} \tag{15}$$

$$-A_m = \frac{R_2}{2R_1} \tag{16}$$

$$Q = \pi f_m R_2 C \tag{17}$$

$$B = \frac{1}{\pi R_2 C} \tag{18}$$

To attain desired filtering performance, the above design parameters should be set as f_m = 60[Hz], B = 5[Hz], Am = −1. Choosing capacitor value C1 = C2 = C = 100[nF] in the circuit diagram of Fig. 2, and using (15)~(18), values of resistors can be determined as R1 = 316[kΩ], R2 = 638[kΩ], and R3 = 1.105[kΩ].

Output of this band-pass filter $i_1(t)$ is a pure sine wave of fundamental frequency (60[Hz]) which is phase shifted by 180[°] with respect to the original fundamental component contained in $i(t)$.

$i_1(t)$ is then fed to a Zero Crossing Detector (ZCD) whose circuit diagram and input/output characteristics are displayed in Fig. 3.
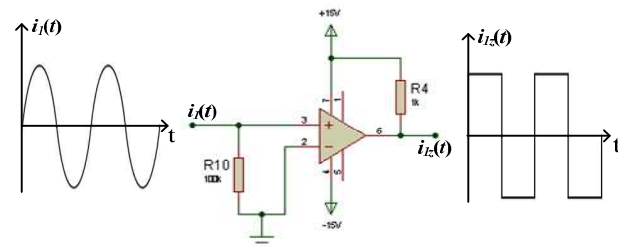

Fig. 3. Circuit diagram with input output waveform of the Zero Crossing Detector (ZCD)

Output $i_{1z}(t)$ obtained from ZCD is further passed through a clipper circuit to get a unipolar signal

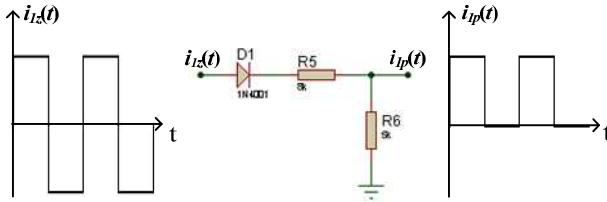$i_{Ip}(t)$ as illustrated in Fig. 4.

Fig. 4. Clipper circuit with input output characteristics

Pulse wave $i_{Ip}(t)$ is connected to the clock input of a D flip-flop through an inverted buffer. This inversion compensates the 180[°] phase shift that occurred previously by the band-pass filter.

On the other hand, system voltage, considered to be containing no harmonic components [20], is sensed by a potential transformer (PT) (Fig. 1) and passed through similar ZCD and clipper section as discussed above. Output of clipper $v_p(t)$ is fed to a D flip-flop as D input through a buffer.

The flip-flop is clocked by current pulse while D input is fed by voltage pulse which results in latching the voltage polarity at the current zero crossing. Output of D flip-flop $D_Q(t)$ can be interpreted as follows.

$$D_Q(t) = \begin{cases} 1; & \text{PF lagging} \\ 0; & \text{PF leading} \end{cases}$$
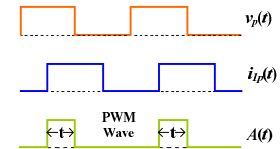
$v_p(t)$ and $i_{Ip}(t)$ are then applied to an AND gate, and pulse wave $A(t)$ is obtained as an output whose width is varied with respect to PF. The relationship between this pulse width modulated (PWM) wave and PF is demonstrated in Fig. 5.
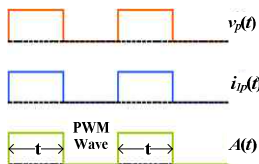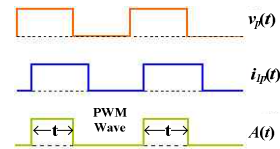
Fig. 5. Generation of PWM wave, (a) at $\theta_1 = 0[°]$ (PF=1), (b) at $\theta_1 = 45[°]$ (PF=0.7), (c) at $\theta_1 = 90[°]$ (PF=0)

The two signals, $D_Q(t)$ and $A(t)$, are then fed to a microcontroller port for further processing and decision. Inside the microcontroller $D_Q(t)$ is used for deciding whether PF is leading or lagging, whereas pulse duration **t**, as shown in Fig. 5, is calculated in seconds to determine DPF expressed below.

$$DPF = \cos\left\{2\pi f\left(\frac{1}{120} - t\right)\right\} \tag{19}$$

Here, f represents frequency of power system which is considered to be 60[Hz] in the calculation.

Two RMS to DC converters IC are employed in this design to get I_1 and I_{rms} which can be expressed by (20) and (21) respectively.

$$I_1 = \frac{I_m}{\sqrt{2}}; \text{ where } I_m \text{ is the peak value of } i_1(t) \tag{20}$$

$$I_{rms} = \sqrt{I_0^2 + I_1^2 + I_2^2 + \ldots + I_n^2} \tag{21}$$

The ripple contained in the output of RMS to the DC converter can be reduced by further passing it through a 2nd order active-RC filter shown in Fig. 6 [28].
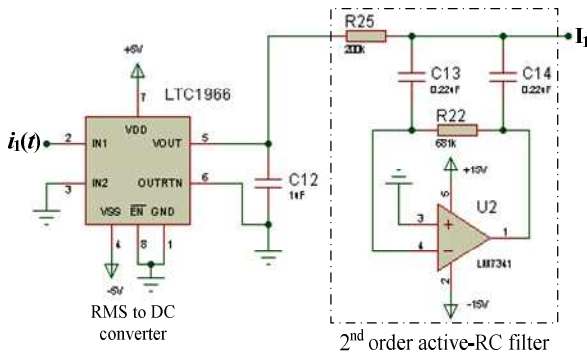
Fig. 6. RMS to DC Converter with post filter

Filtered outputs I_1 and I_{rms} are then applied to the
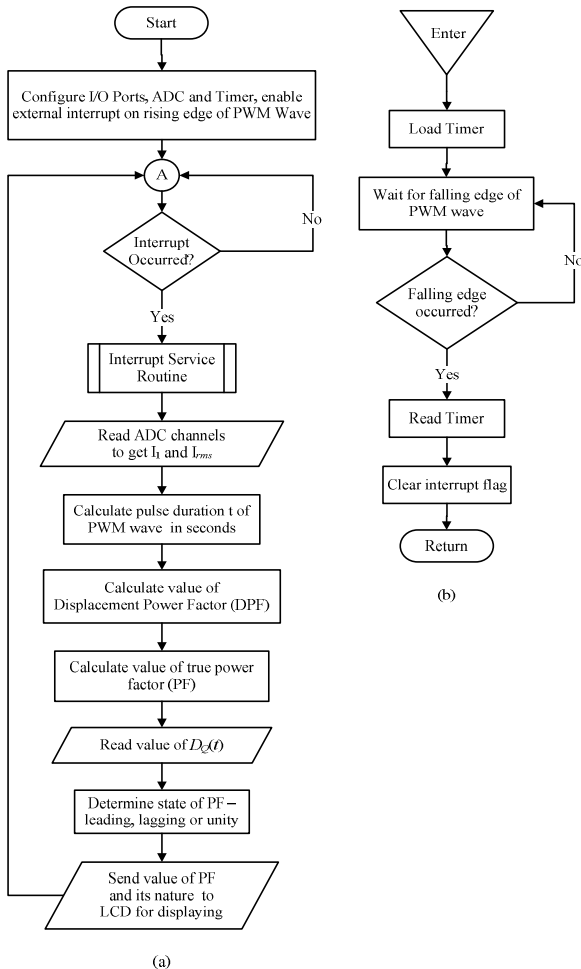

(a)

Fig. 7. Flow charts for programs. (a) main
program; (b) interrupt service routine

ADC channels of a microcontroller for A/D conversion. The digital value that results is used afterwards for determining PF value according to expression (9).

A LCD, driven by microcontroller, can display the real time value of PF as well as its lead/lag nature.

4. Algorithm for PF Measurement

Simplified flowcharts of the implemented algorithm are described in Fig. 7. The PWM wave is treated as an external interrupt signal for the microcontroller. At the rising edge of the PWM wave an interrupt is generated and the main program branches to the interrupt service routine
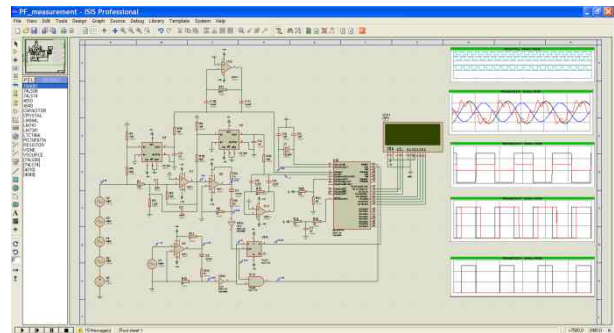

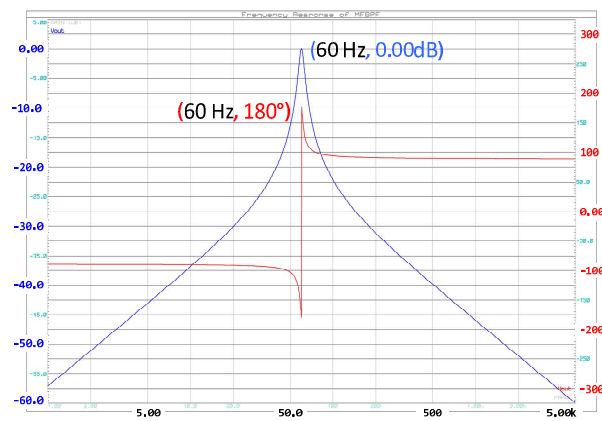Fig. 8. Simulation environment in Proteus ISIS

Fig. 9. Frequency response of Multiple Feedback
band-pass filter. (X-axis: frequency in
[Hz], left Y-axis: gain in [dB], right
Y-axis: phase in degree)

(ISR). The interrupt service routine (Fig. 7b) loads the Timer to start measurement of pulse duration. On the falling edge of the PWM wave the Timer is stopped and the timer register is read. This timing data along with ADC channels' readings is used for calculating a true power factor. Lead/lag discrimination is obtained by the input state of $D_Q(t)$.

5. Simulation Results and Performance Analysis

The design and simulation of the proposed method are performed by Proteus ISIS which uses the SPICE3f5 analogue simulator kernel with a fast event-driven digital simulator to provide seamless mixed-mode simulation [29]. It has the ability to simulate interaction between software running on a microcontroller and any analog or digital electronics connected to it. Fig. 8 shows the simulation environment in Proteus ISIS.

Frequency response (Fig. 9) of the multiple feedback band-pass filter confirms its effectiveness in eliminating all the harmonic components contained in the distorted current wave.

Waveforms obtained by simulation for a test case (THD=113.12[%] and $i(t)$ containing odd harmonics up to 33rd order) is illustrated in Fig. 10 where the signal labels correspond to that of Fig. 1. Here, Total Harmonic Distortion (THD) is defined as [7, 21, 22, 25]

$$\%\,THD = \frac{I_{dis}}{I_1} \times 100 \qquad (22)$$

where I_1 is the rms value of the fundamental component and I_{dis} is the rms value of the total harmonic component.
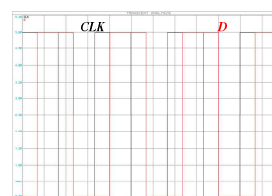
Simulation is performed for different values of

THD and harmonic contents. The values of PF that were obtained are then compared to the theoretical ones and a percentage of errors is calculated. Simulation results, as shown in Table 1, justify the effectiveness of the proposed method for measuring PF and its nature under nonlinear load current
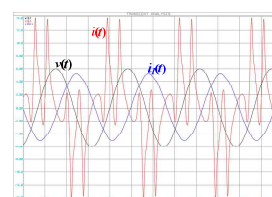
(a)
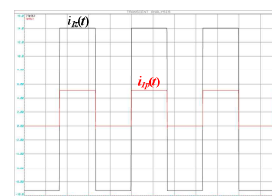
(b)
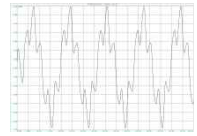
(c)
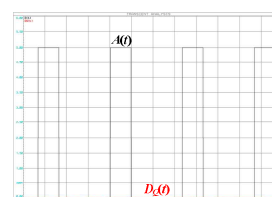
(d)

Fig. 10. Simulated output for THD = 113.12[%] while $i(t)$ contained odd harmonics up to 33rd order. (a) System voltage $v(t)$, load current $i(t)$ and output of band-pass filter $i_1(t)$, (b) output of ZCD $i_{1z}(t)$ and clipper $i_{1p}(t)$, (c) CLK and D input of D flip-flop, (d) PWM wave $A(t)$ and lead/lag indicator signal $D_Q(t)$

Table 1: Comparison of theoretical and simulation results(L$_d$=PF leading; L$_g$=PF lagging, T=theoretical)

THD (%)	I$_0$ (A)	Peak value of i$_1$(t) (A)	Harmonics in i(t)	Example waveform	PF (Theoretical)	PF (Simulation)	%Error
6.40	0.05	10	5th 7th 11th		0.9639L$_g$	0.9695L$_g$	0.58
					0.8642L$_d$	0.8684L$_d$	0.48
					0.7056L$_g$	0.7235L$_g$	2.53
					0.4990L$_d$	0.516L$_d$	3.41
				For PF = 0.7056L$_g$(T)	0.1733L$_g$	0.1782L$_g$	2.83
35.76	0.1	5	5th 7th 11th		0.9413L$_g$	0.9475L$_g$	0.66
					0.8152L$_d$	0.8207L$_d$	0.68
					0.6656L$_g$	0.6677L$_g$	0.32
					0.4706L$_g$	0.4877L$_g$	3.63
				For PF = 0.4706L$_g$(T)	0.1634L$_d$	0.1684L$_d$	3.03
104	0.01	2.55	3rd 5th 7th		0.6694L$_d$	0.6853L$_d$	2.37
					0.6002L$_g$	0.6101L$_g$	1.65
					0.4900L$_d$	0.4842L$_d$	1.19
					0.3465L$_g$	0.333L$_g$	3.9
				For PF = 0.6694L$_d$(T)	0.1794L$_g$	0.175L$_g$	2.43
140.1	0.002	2.85	3rd 5th 7th		0.5612L$_g$	0.5691L$_g$	1.42
					0.5031L$_d$	0.5039L$_d$	0.16
					0.4108L$_g$	0.3999L$_g$	2.65
					0.2905L$_d$	0.2889L$_d$	0.54
				For PF = 0.1504L$_g$(T)	0.1504L$_g$	0.1453L$_g$	3.37
54.56	0.01	10	3rd to 19th (odd ones only)		0.8745L$_g$	0.8822L$_g$	0.88
					0.7602L$_g$	0.7761L$_g$	2.09
					0.6207L$_g$	0.6379L$_g$	2.77
					0.4389L$_g$	0.455L$_g$	3.67
				For PF = 0.2272L$_d$(T)	0.2272L$_d$	0.2196L$_d$	3.34
194.01	0.01	5	3rd to 19th (odd ones only)		0.4564L$_d$	0.4566L$_d$	0.04
					0.3968L$_g$	0.3963L$_g$	0.12
					0.3240L$_g$	0.3301L$_g$	1.89
				For PF = 0.2291L$_g$(T)	0.2291L$_g$	0.2375L$_g$	3.68
113.12	0.01	5	3rd to 33rd (odd ones only)		0.6598L$_g$	0.6677L$_g$	1.2
					0.5736L$_g$	0.5712L$_g$	0.42
					0.4683L$_g$	0.4714L$_g$	0.66
					0.3312L$_d$	0.3304L$_d$	0.23
				For PF = 0.1714L$_d$(T)	0.1714L$_d$	0.1662L$_d$	3.05

condition with less than 4[%] error.

6. Conclusion

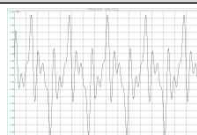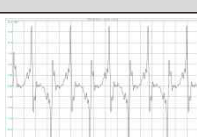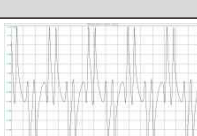The proposed method for measuring power factor (PF) and its nature under nonlinear load current situation appears to be efficient, simple, and cost effective. Its accuracy was confirmed by simulation. The method is competitive with methods followed by commercially available equipment for the same purpose.

This method has the ability to measure PF under both sinusoidal and non-sinusoidal situations. Hence, it can be utilized for monitoring and control of PF and other related power parameters in a large electrical system.

Our future research will focus on hardware implementation of the proposed design. We plan to evaluate its performance in situations where we have to deal with issues like current and potential transformer saturation, input saturation of RMS to DC converter IC, and accurate generations of current harmonics and precise implementations of band-pass filters.

References

[1] Weinian Tan and Vilayil I. John , "Nonlinear fluorescent systems: their impact on power quality," Proceedings of Canadian Conference on Electrical and Computer Engineering, vol. 1, pp. 144 - 147, September 1994.

[2] K.C. Umeh, A. Mohamed, R. Mohamed, "Comparing the harmonic characteristics of typical single-phase nonlinear loads," Proceedings of National Power and Energy Conference (PECon) 2003 , Bangi, Malaysia, pp. 383-387, December 2003.

[3] K. Johonson and R. Zavadil, "Assessing the impacts of nonlinear loads on power quality in commercial building— An overview," in Conference Record, IEEE Industry Applications Society Annual Meeting, vol. 2, pp. 1863 - 1869, 1991.

[4] S. Kamakshaiah, J. Amarnath, Pannala Krishna Murthy, S. Kamakshaiah, Pannala Krishna Murthy, J. Amarnath, Electrical Measurements and Measuring Instruments, I. K. International Publishing House Pvt. Ltd, pp. 68-85, 2010.

[5] Daniel Slomovitz, "Behaviour of power-factor meters under non-sinusoidal current and voltage," International Journal of Electronics, Vol. 70, No. 4, pp. 827 - 838, 1991.

[6] J. C. Wu and H. L. Jou, "Fast response power factor detector," IEEE Transactions on Instrumentation & Measurement, vol. 44, No. 4, pp. 919 - 922, Aug. 1995.

[7] Kuen-Der Wu, Hurng-Liahng Jou, and Jhy-Shoung Yaung, "A New Circuit for Measuring Power Factor in Nonsinusoidal Load Current," IEEE Transactions on Industrial Electronics, vol. 46, No. 4, pp. 861 - 864, August 1999.

[8] Petar N. Miljanic, Borislav Stojanovic, Vladimir Petrovic, "A Novel Method for the Measurement of Power, Power Factor, rms, and Average Values of Voltage and Current of Distorted Power Frequency Waves, " IEEE Transactions on Instrumentation and Measurement, Vol. 29, No. 4, pp. 432-434, December 1980.

[9] A. Kuppurajulu, P.C. Majhee, C. Venkataseshaiah, "A Fast Response Device for Measurement of Power, Reactive Power, Volt-Amperes and Power Factor," IEEE Transactions on Power Apparatus and Systems, Vol. PAS-90, No.1, pp. 331-338, January 1971.

[10] D. R. Tutakne, H. M. Suryawanshi, T. G. Arora, Mahesh Mishra, S. G. Tarnekar, "Single-Phase Fast Response Power Factor Transducer," IEEE International Symposium on Industrial Electronics (ISIE'06), pp. 1765 - 1768, July 9-13, 2006.

[11] J. Gou, B. Xie, P. Enjeti, "A DSP based real time power quality measurement system," Proceedings of IEEE Applied Power Electronics Conference and Exposition (APEC '92), pp. 299-302, 23-27 February 1992.

[12] J.-C. Montano, A. Lopez, M. Castilla, J. Gutierrez, "DSP-based algorithm for electric power measurement," IEE Proceedings Science, Measurement and Technology, Vol. 140, No. 6, pp. 485-490, November 1993.

[13] A. Ozdemir, A. Ferikoglu, "Low cost mixed-signal microcontroller based power measurement technique," IEE Proceedings- Science, Measurement and Technology, Vol. 151, No. 4, pp. 253-258, July 2004.

[14] Shu-Chen Wang, Chi-Jui Wu, "Design of Accurate Power Factor Measurement Approach Using FPGA-based Chip," WSEAS Transactions on Circuits and Systems, Vol. 9, NO. 7, July 2010.

[15] Voltech Instruments Ltd., "PM3000 User Manual," Ver. 10, pp. 1-3, 2002.

[16] A.A. Girgis, F.M. Ham, "A Quantitative Study of Pitfalls in the FFT," IEEE Transactions on Aerospace and Electronic Systems, Vol. AES-16, No.4, pp.434-439, July 1980.

[17] L. Angrisani, P. Daponte, M. D'Apuzzo, A. Testa, "A measurement method based on the wavelet transform for power quality analysis," IEEE Transactions on Power Delivery, Vol. 13, No. 4, pp. 990-998, October 1998.

[18] A. Sarkar, S. Sengupta, "A novel instantaneous power factor measurement method based on wavelet transform," Proceedings of IEEE Power India Conference, pp. 6-11, April 2006.

[19] T. Manmek, C. Grantham, T. Phung, "A new efficient algorithm for online measurement of power system quantities," Proceedings of 30th Annual Conference of IEEE Industrial Electronics Society, (IECON 2004), Vol.2, pp. 1184-1189, 2-6 November 2004.

[20] Indrajit Purkayastha, Paul J. Savoie, "Effect of Harmonics on Power Measurement," IEEE Transactions on Industry Applications, vol. 26, No. 5, pp. 944 - 946, September/October 1990.

[21] N. Mohan, T. M. Undeland, and W. P. Robbins, Power Electronics: Converter Applications and Design, 2nd ed., John Wiley & Sons Inc, pp. 33-43, 1995.

[22] IEEE Standard 1459-2000, "IEEE Trial-Use Standard Definitions for the Measurement of Electric Power Quantities Under Sinusoidal, Non-sinusoidal, Balanced, Or Unbalanced Conditions," pp. i-44, 2002.

[23] L.X. Zhou, Z.D. Yin, X.N. Xiao, Z.Q. Wang and L. Zheng, "Study on Power Factor Through the Similarity of Waveform", 3rd IEEE Conference on Industrial Electronics and Applications, ICIEA 2008, Vol.2, pp. 1534-1537, 2008.

[24] Bogdan Spasojević, "The Time Domain Method for Power Line Reactive Energy Measurement", IEEE Transactions on Instrumentation and Measurement, Vol. 56, No. 5, pp. 2033-2042, October 2007.

[25] Alexander Eigeles Emanuel, "Summary of IEEE Standard 1459: Definitions for the Measurement of Electric Power Quantities Under Sinusoidal, Nonsinusoidal, Balanced, or Unbalanced Conditions," IEEE Transactions on Industry Applications, Vol. 40, No. 3, pp. 869-867, May/June 2004.

[26] P. S. Filipski, Y. Baghzouz and M. D. Cox, "Discussion of Power Definitions Contained in The IEEE Dictionary," IEEE Transactions on Power Delivery, Vol. 9, No. 3, pp 1237-1243, July 1994.

[27] Ron Mancini Ed., "Op Amps for Everyone," Texas Instruments, Design Reference, SLOD006B, pp. 16-27 - 16-36, August 2002.

[28] Linear Technology, "LTC 1966 Datasheet," pp. 18, 2004.

[29] Labcenter Electronics, "What is Proteus VSM," available at: http://www.labcenter.com/products/vsm_overview.cfm, accessed on 5th September, 2011.

[30] IEEE Working Group on Nonsinusoidal Situations: Effects on Meter Performance and Definitions of Power, "Practical definitions for powers in systems with nonsinusoidal waveforms and unbalanced loads: a discussion," IEEE Transactions on Power Delivery, vol. 11, no. 1, pp. 79-101, January 1996.

[31] C. Venkatesh, D. Srikanth Kumar, D.V.S.S. Siva Sarma, M. Sydulu, "Modelling of Nonlinear Loads and Estimation of Harmonics in Industrial Distribution System," Proceedings of Fifteenth National Power Systems Conference (NPSC), pp. 592-597, IIT Bombay, December 2008.

[32] Ming-Yin Chan, Ken KF Lee, Michael WK Fung, "A Case Study Survey of Harmonic Currents Generated from a Computer Centre in an Office Building," Architectural Science Review, Volume 50, No. 3, pp. 274-280, 2007.

[33] W. Mack Grady, Robert J. Gilleskie, "Harmonics and How They Relate to Power Factor," Proceedings of the EPRI Power Quality Issues & Opportunities Conference (PQA'93), pp. 1-8, San Diego, CA, November 1993.

◇ 저자소개 ◇─────────────────────────

Md. Rifat Shahriar
Mar. 2011~Present: Univ. of Ulsan, School of Electrical Eng., Graduate Student. Aug. 2008: Chittagong Univ. of Eng. and Tech., Dept. of Electrical and Electronic Eng., B.Sc. Aug. 2008 ~ Present: International Islamic Univ. Chittagong, Dept. of Electrical and Electronic Eng., Lecturer.
Interests: Digital Signal Processing, Circuits and System Design, Fault Detection and Diagnosis.

Ui-Pil Chong
Dec. 1996: New York Univ. (Polytechnic), Dept. of Electrical and Computer Eng., Ph.D. Jun. 1985: Oregon State Univ., Dept. of Electrical and Computer Eng., MSEE. Feb. 1980: Korea Univ., Dept. of Electrical Eng., M.E. Feb. 1978: Univ. of Ulsan, Dept. of Electrical Eng., B.E. Mar. 1997~Present: Univ. of Ulsan, School of Electrical Eng., Professor.
Interests: Digital Signal Processing, Multimedia, Fault Detection and Diagnosis.